

# Are the existing CMB maps sufficiently accurate for the matched circle test?

H. Then<sup>1</sup>★

<sup>1</sup>Abteilung Theoretische Physik, Universität Ulm, Albert-Einstein-Allee 11, 89069 Ulm, Germany

Received 2005 November 25

## ABSTRACT

WMAP has provided CMB maps of the full sky. But the raw data is subject to foreground contamination, in particular near to the Galactic plane. Foreground cleaned maps have been derived, e.g., the internal linear combination (ILC) map of Bennett et al. (2003), and the reduced foreground TOH map of Tegmark et al. (2003). Using  $S$  statistics we examine the amount of the residual foreground contamination that is left over in the foreground cleaned maps. In particular, we specify which foreground cleaned map is the best to be used in quantitative analyses and discuss whether the CMB fluctuations are known sufficiently accurate in order to find pairs of matched circles in the sky. We generalise the  $S$  statistic, called  $D$  statistic, such that the circle test can deal with CMB maps in which the contaminated regions of the sky are excluded with masks. This increases the chance for the detection of matched circles in the sky. An estimate however shows that even with foreground cleaned CMB maps, where in addition the most noisiest parts of the sky are masked, it is very hard to find matched circles.

**Key words:** methods: data analysis – methods: statistical – cosmic microwave background – large-scale structure of Universe – cosmology: miscellaneous

## 1 INTRODUCTION

Astronomical observations of recent years have answered a number of fundamental questions. A cornerstone in *revealing the state of the universe* was the combination of observations at low redshift (clusters, including the mass-to-light method, baryon fraction, and cluster abundance evolution), intermediate redshift (SNe), and high redshift (CMB) (Bahcall et al. 1999). On the other hand, many new fundamental questions were raised, e.g., questions concerning dark matter and dark energy. Moreover, many answers depend sensitively on the accuracy of the observations, e.g., on the accuracy of the curvature which determines whether we live in an *exactly* flat universe or a slightly curved one.

Concerning the high redshift observations, the temperature fluctuations in the CMB are subject to systematic errors resulting from foreground contamination. In particular near to the Galactic plane, the CMB maps are highly contaminated by radiation from the Milky Way. Fortunately, there exist methods to reduce the foreground contamination in the maps (Tegmark & Efstathiou 1996; Bennett et al. 2003). A growing number of foreground cleaned maps are available (Bennett et al. 2003; Tegmark, de Oliveira-Costa & Hamilton 2003; Eriksen et al. 2004) and the reader may ask which of them comes closest to the genuine temperature fluctuations of the CMB. This question is related to the question how reliable the maps are, especially near to the Galactic plane. There is

no way to decide whether a given pixel of a map displays the correct temperature (apart from pixels that are really very off in their values), because the genuine temperature fluctuations of the CMB are unknown. But taking ensembles of pixels, it is possible to check statistically whether the spatial temperature distribution agrees with statistical isotropy. In this paper we perform such checks using  $S$  statistic and a generalisation of it. The result is that even for the best available CMB map there is left residual foreground contamination. Because of this residual foreground contamination, we extend the definition of the  $S$  statistic such that the foreground contaminated regions of the sky can be excluded. This opens a new chance for the detection of matched circles as a result of the non-trivial topology of the universe (Cornish, Spergel & Starkman 1998). However, estimating the expected peak values in the  $S$  and in the more general  $D$  statistic for matched circles leads to a strong conclusion concerning the tests that have been done so far (de Oliveira-Costa et al. 2004; Cornish et al. 2004; Roukema et al. 2004; Aurich, Lustig & Steiner 2005c).

## 2 D STATISTIC

$S$  statistic was initially introduced by Cornish et al. (1998) for the search of correlated pairs of circles in the CMB sky.

$$S = \frac{\langle 2\delta T_1(\pm\phi)\delta T_2(\phi + \phi_*) \rangle}{\langle \delta T_1(\phi)^2 + \delta T_2(\phi)^2 \rangle}, \quad (1)$$

★ E-mail: holger.then@uni-ulm.de

## 2 H. Then

where  $\delta T_i(\phi)$  ( $i = 1, 2$ ) denotes the CMB temperature fluctuations on two circles 1 and 2, and  $\langle \cdot \rangle = \int_0^{2\pi} d\phi$  is the integration along the two circles of equal radius with relative phase  $\phi_*$ .

We generalise the definition of the  $S$  statistic to include weights that specify the certainty resp. uncertainty of the temperature fluctuations. The new statistic is called  $D$  statistic. In addition, we note that the  $D$  statistic is not restricted to correlations along circles, but can be used along arbitrary curves  $\gamma$ .

**Definition 1.** Let  $\gamma_1$  and  $\gamma_2$  be curves parametrized by  $\phi$ ,  $\phi \in [0, 2\pi]$ , and  $w(\gamma_i)$  be positive weights that specify how accurate the CMB temperature fluctuations  $\delta T(\gamma_i)$  are known at  $\gamma_i = \gamma_i(\phi)$ . Using the notation

$$\langle\langle f(\gamma_1, \gamma_2) \rangle\rangle := \int_0^{2\pi} d\phi f(\gamma_1(\phi), \gamma_2(\phi)) \times \times \sqrt{w(\gamma_1(\phi))w(\gamma_2(\phi))|\frac{d}{d\phi}\gamma_1(\phi)||\frac{d}{d\phi}\gamma_2(\phi)|},$$

we call

$$D := \frac{\langle\langle \delta T(\gamma_1)\delta T(\gamma_2) \rangle\rangle}{\langle\langle \delta T(\gamma_1)^2 + \delta T(\gamma_2)^2 \rangle\rangle} \quad (2)$$

$D$  statistic.

We remark that the  $D$  statistic is invariant if the weights are rescaled, i.e.,  $w(\gamma_i(\phi)) \mapsto cw(\gamma_i(\phi))$ , where  $c$  is a positive constant. The same is also true if the temperatures are rescaled.

The weights may be expressed by  $w = (1 + 1/\xi)^{-1}$ , where  $\xi$  is the signal-to-noise ratio. If a temperature fluctuation is known exactly, the corresponding weight equals 1. In the other extreme, i.e., when  $\delta T$  is not known at all, its weight vanishes.

It is allowed to parametrize the curves  $\gamma_i$  arbitrarily, but care has to be taken if the ratio between  $|\frac{d}{d\phi}\gamma_1(\phi)|$  and  $|\frac{d}{d\phi}\gamma_2(\phi)|$  varies with  $\phi$ , because the  $D$  statistic depends on the parametrization. We will always choose the parametrization such that  $|\frac{d}{d\phi}\gamma_i(\phi)| = \text{const}$  allowing us to drop the factors  $|\frac{d}{d\phi}\gamma_i(\phi)|$  in the definition of the  $D$  statistic.

If one chooses the curves  $\gamma_1$  and  $\gamma_2$  to be circles of the same radius and sets all weights equal to 1, one recovers (1) as a special case of (2).

The  $D$  statistic always takes values between  $D = -1$ , maximal *anticorrelation*, and  $D = 1$ , maximal *correlation*. In a typical resolution-limited application the  $D$  statistic has a value distribution that is centred near

$$D_{\text{peak}} = \frac{\chi^2}{1 + \chi^2} \quad (3)$$

and has

$$\text{FWHM} \simeq \sqrt{\frac{8 \ln 2}{N_0}} \quad (4)$$

for  $N_0$  large, where  $N_0$  is the number of *independent* pixels (Cornish et al. 1998).  $\chi$  is the correlation ratio,

$$\chi^2 = \frac{A_{\text{corr}}^2}{A^2 - A_{\text{corr}}^2}, \quad (5)$$

where  $A_{\text{corr}}$  stands for the mean amplitude of the correlated part of the signal, and  $A$  for the mean amplitude of the total signal including the detector noise, i.e.,  $A^2 = A_{\text{corr}}^2 + A_{\text{uncorr}}^2 + A_{\text{noise}}^2$ .

## 3 THE METHOD

Observing the CMB over the full sky, one is confronted with foreground emission of our own galaxy that strongly contaminates the

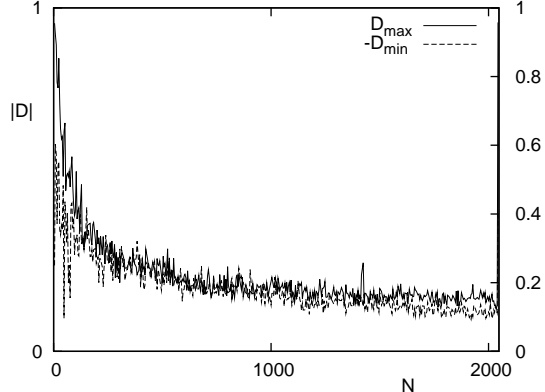


**Figure 1.**  $D$  statistic of the foreground cleaned  $W$ -band map where the extremal  $D$ -values, i.e.  $D_{\text{max}}$  and  $-D_{\text{min}}$ , are plotted for front-to-front circles that are parallel to the Galactic plane.  $N$  is the length of the circles in number of HEALPIX pixels. All front-to-front circles that are close to the Galactic plane have the same ‘length’ of  $N = 2048$  pixels. Therefore, the Galactic foreground contamination is not displayed. The extragalactic contamination is quite negligible, since it does not destroy the symmetry between  $D_{\text{max}}$  and  $D_{\text{min}}$ , except for some  $D$ -values of small circles near to the poles and of large circles that come close to the equatorial zone.

temperature fluctuations near to the Galactic plane. A quantitative measure of this foreground contamination can be obtained from the  $D$  statistic by choosing  $\gamma_1$  to be a closed path and setting  $\gamma_2(\phi) = \gamma_1(\phi_* - \phi)$ . In the subcase of circles we call this setup *front-to-front* circles, because  $\gamma_2$  traverses the same circle as  $\gamma_1$ , but in the opposite direction.

Our working hypothesis is that for almost points on the sky there are temperature fluctuations in the CMB on all scales and that the cosmological principle holds. Consequently, we do not expect any correlations in the genuine temperature fluctuations, i.e.  $A_{\text{corr}} = 0$ , apart from the circle-in-the-sky signature in case of a non-trivial topology of the universe. In other words, the typical temperature fluctuations of the CMB should result in a  $D$  statistic that is symmetric around  $D_{\text{peak}} = 0$ . That this expectation indeed holds is shown with front-to-front circles that are far away from the Galactic plane, see Fig. 1. (All figures in this section, namely Figs. 1–3, were made with the foreground cleaned  $W$ -band map of the first year  $WMAP$  data (Bennett et al. 2003). More details about the CMB maps can be found in Sec. 4.) What we actually plot in Fig. 1 is not a histogram of the  $D$ -values, but  $-D_{\text{min}} := -\min_{\phi_*} D$  and  $D_{\text{max}} := \max_{\phi_*} D$  in dependence of the ‘circle length’  $N$ , where  $N$  is the length of the front-to-front circles measured in number of HEALPIX pixels,  $N$ , which is not equal to the number of independent pixels,  $N_0$ , on the paths. Being symmetric around  $D_{\text{peak}} = 0$ , the smallest and largest quantities of a finite set of  $D$ -values have similar size, except of their opposite signs, i.e.,  $-D_{\text{min}} \approx D_{\text{max}}$ . In short, we call this to be a *symmetry* between  $D_{\text{min}}$  and  $D_{\text{max}}$ . In Fig. 1 we see also that the width of the distribution which is related to the sum of  $-D_{\text{min}} + D_{\text{max}}$  decreases monotonically with increasing length  $N$  of the circles, apart from statistical fluctuations. This is in agreement with Eq. (4), since larger circles sample more independent pixels. On the other hand, front-to-front circles that cross the Galactic plane perpendicular reveal strong correlations resulting from foreground contamination, see Fig. 2. Both, the symmetry between  $D_{\text{min}}$  and  $D_{\text{max}}$ , and the monotonically decreasing sum  $-D_{\text{min}} + D_{\text{max}}$  are heavily distorted by peaks in  $D_{\text{max}}$  that result from residual foregrounds. Figure 3

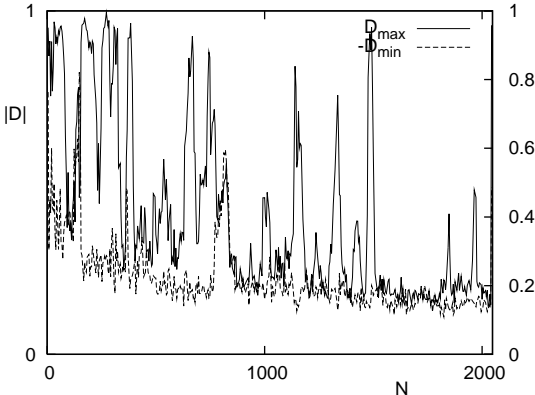


**Figure 2.**  $D$  statistic of the foreground cleaned  $W$ -band map where the front-to-front circles cross the Galactic plane perpendicular. The peaks in  $D_{\max}$  and the asymmetry between  $D_{\max}$  and  $D_{\min}$  result from Galactic foreground contamination.

looks completely different to the former. The only difference in producing it, was to apply a galaxy cut. While in Fig. 2 all weights were set equal to 1, in Fig. 3 those inside the Kp4 mask of Bennett et al. (2003) were set to zero which is tantamount to taking only those parts of the circles that are outside the galaxy cut. We do not count the pixels that are inside the galaxy cut. This is the reason why in Fig. 3 there are no circles with  $N > 1992$ . The symmetry between  $D_{\min}$  and  $D_{\max}$ , and the monotonically decreasing width of the distribution in Fig. 3 show that there is far less contamination outside the Kp4 mask. The Figs. 2–8 were all made with the same front-to-front circles, i.e., circles that cross the Galactic plane perpendicular. It is therefore possible to compare these figures directly with each other.

Of interest to the current paper are also the other foreground reduced maps, i.e., the ILC, the LILC, and the two TOH maps. We question how reliable these maps are, in particular near to the Galactic plane. With reliable we mean whether there are any correlations from foreground contamination or any systematics from the process of creating the maps. We emphasize that *not all* foreground systematics necessarily result in correlations. For example uncorrelated gaussian noise that contaminates the data will never be recovered with the  $D$  statistic. But turning the tables, as soon as we find any correlation, we doubt that the temperature fluctuations are free of residual foreground systematics. Applying masks allows us to locate the foreground contaminated regions. The only exception are correlations according to the circle-in-the-sky signature. If present, one can circumvent the latter in choosing paths that are not circles.

#### 4 CMB MAPS

The following foreground reduced CMB maps are available from the LAMBDA archive:

- (a) The foreground cleaned  $Q$ -,  $V$ -, and  $W$ -bands of the first year *WMAP* data (Bennett et al. 2003) that result from removing the free-free, synchrotron, and dust emissions via externally derived CMB template fits. The advantages of these maps are the high resolution, in particular 0.23 degree for the  $W$ -band, the well-specified noise properties, and the frequency specific information that is contained in the three microwave bands,  $Q$ ,  $V$ , and  $W$ .
- (b) The internal linear combination (ILC) map that is designed

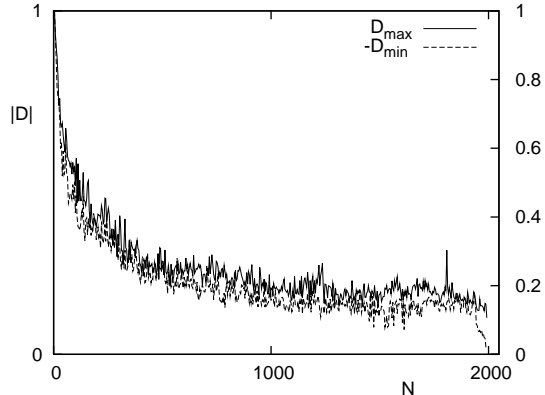


**Figure 3.** The same as in Fig. 2, except that the Kp4 mask has been applied. This shows that there is far less foreground contamination outside the Kp4 mask.

to reduce the foreground contamination via weighted combinations of the five *WMAP* bands (Bennett et al. 2003).

(c) The LILC map of Eriksen et al. (2004) produced with a variant of the ILC algorithm that employs a Langrange multiplier.

(d) The reduced foreground TOH map of Tegmark et al. (2003) that results from a variant of the Tegmark & Efstathiou (1996) technique that is completely unbiased, making no assumptions about the CMB power spectrum, the foregrounds, the *WMAP* detector noise or external templates. Since the TOH map is free of assumptions about external templates, it has the advantage that it can be used for cross-correlation with, e.g. galaxy and  $X$ -ray maps. Furthermore, according to Tegmark & Efstathiou (1996) their technique preserves the information on the noise properties of the CMB map. In principle, Tegmark et al. (2003) should be able to specify the noise properties of their map. But unfortunately, there are no noise properties given for the TOH map.

(e) The Wiener filtered TOH map (Tegmark et al. 2003) which is designed for visualisation purposes in order to represent the best guess as to what the CMB sky actually should look like.

Applying the  $D$  statistic to these maps, we find:

(a) The foreground cleaned  $Q$ -,  $V$ -, and  $W$ -band maps are useful for quantitative analyses outside the Kp4 mask, see Fig. 3 and the text in Sec. 3. Since the templates were fit only with data outside the Kp2 mask and the foreground removal is not applicable to regions near to the Galactic plane where the spectrum of the Galactic emission is different, these maps should never be used inside the Kp4 mask, see Fig. 2.

(b) According to Bennett et al. (2003) the ILC map is useful for visual presentation of the CMB anisotropy signature and for foreground studies. However, because of the complicated noise correlations, it should not be used for CMB studies. Our findings agree with this statement. The distribution of the  $D$  statistic is very wide, see Fig. 4. The large values of  $-D_{\min}$  and  $D_{\max}$  highlight the low resolution of the ILC map, cf. Eq. (4) and the text in Sec. 3. Furthermore, the  $D$  statistic is not symmetric around  $D_{\text{peak}} = 0$ . The asymmetry between  $D_{\min}$  and  $D_{\max}$  indicates that some residual foreground systematics are present in the ILC map. At least the Kp4 mask has to be applied in order to remove the asymmetry.

(c) The LILC map shows similar results as the ILC map, see Fig. 5. This means that it should not be used for quantitative CMB studies.

(d) The  $D$  statistic reveals that the TOH is better than all other

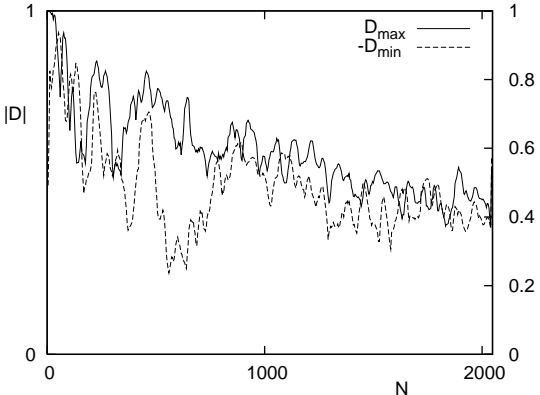


**Figure 4.**  $D$  statistic of the ILC map. The large values of  $D_{\max}$  and  $-D_{\min}$  highlight the low resolution of the ILC map. The asymmetry between  $D_{\max}$  and  $D_{\min}$  indicates that foreground systematics are present.

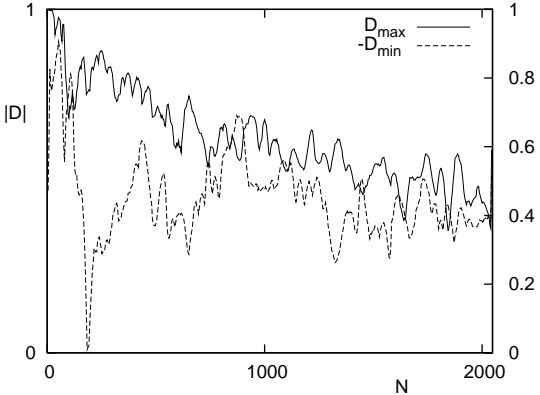


**Figure 5.**  $D$  statistic of the LILC map.

maps, if one analyses the full sky without any cut, see Fig. 6. But still, there are foreground systematics present that require the Kp4 mask to be applied, see Fig. 7. If compared to the foreground cleaned  $W$ -band map of Bennett et al. (2003), see Fig. 3, the distribution of the  $D$  statistic is slightly wider for the TOH map indicating that the resolution is slightly worse than the claimed 13 arcmin. There is one sharp peak in Fig. 7 at  $N = 1808$ . Less pronounced, this peak occurs also in Fig. 3. The reader however is warned not to misinterpret this peak as a detection of a matched circle pair. If the Kp4 mask combined with the point source mask of Bennett et al. (2003) is applied, the sharp peak in Fig. 7 vanishes completely. This tells us that there is some residual foreground contamination outside the Kp4 mask, but inside the point source mask.

(e) Our findings show that the Wiener filtered TOH map has a low resolution according to the large width of the distribution in Fig. 8. In addition, the Kp4 mask is required to remove the asymmetry in the  $D$  statistic.

## 5 TOPOLOGY AND CIRCLES IN THE SKY

In the following we choose the foreground cleaned  $W$ -band of Bennett et al. (2003) and use the matched circle test in order to search for signatures of a non-trivial topology. Such searches have already been done for back-to-back (de Oliveira-Costa et al. 2004;

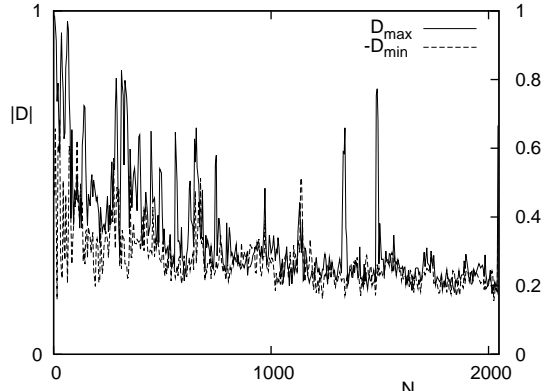


**Figure 6.**  $D$  statistic of the TOH map.

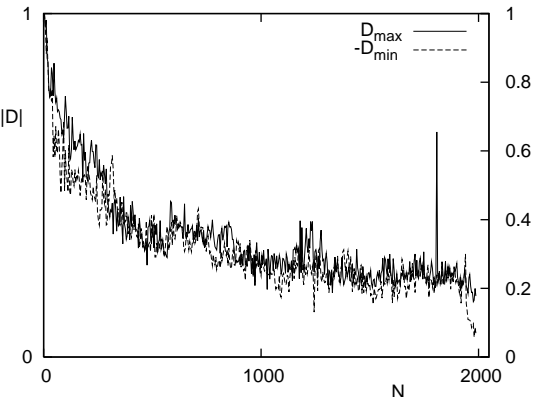


**Figure 7.**  $D$  statistic of the TOH map outside the Kp4 mask.

Roukema et al. 2004; Aurich et al. 2005c) and nearly back-to-back circles (Cornish et al. 2004).

Since Cornish et al. (2004) have not found any matched circle pair, one could conclude that the universe has a trivial topology. At this point it is worthwhile to remember that Roukema et al. (2004) have reported a slight signal for six circle pairs with a radius of  $11 \pm 1$  degree in the ILC map which they interpret as a possible hint for the left-handed dodecahedral space. While the systematic research for matched circles in spherical spaces carried out by Aurich et al. (2005c) has not found these circles, Aurich et al. (2005c) however report a marginal hint for the right-handed dodecahedron and for the right-handed binary tetrahedral space, respectively. In addition, there is strong evidence for a finite universe with a small dimension, because of the anomalies of the large scale temperature fluctuations which rule out the concordance model with a probability of 99.996 per cent, but could be explained by a multiply connected universe (de Oliveira-Costa et al. 2004). These anomalies are the surprisingly low quadrupole, the quadrupole-octupole alignment, and the planar octupole.

We are not aiming to repeat a back-to-back search. We avoid also to run the full search that has been started by Cornish et al. (2004), because this would require more computer resources than we could ever afford. Instead, we explore whether there are any matched front-to-front circles in the sky. This search has never been carried out before, and it can be done within four weeks on a multiprocessor workstation. In our search we exclude contaminated regions of the CMB sky via the Kp4 mask and the point source mask

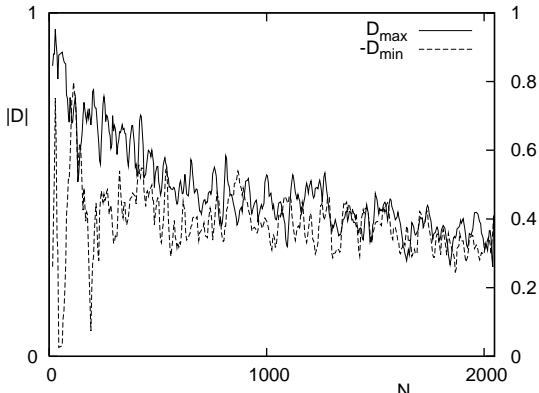


Figure 8.  $D$  statistic of the Wiener filtered TOH map.

by setting the weights inside these masks equal to zero and outside equal to 1, see the equations in Def. 1.

One may wonder whether it makes sense to search for front-to-front circles. Are there any topologies that predict front-to-front circles? The surprising answer is *yes*. An example is the Picard universe (Aurich et al. 2004). Choosing the cosmological parameters as was done in Aurich et al. (2004, 2005a) the Picard universe predicts 40 circle pairs of which 23 are front-to-front. Further details of the Picard topology can be found in Aurich, Steiner & Then (2003); Then (2006). Not only the Picard, but also many other topologies in spherical, flat, and hyperbolic space, respectively, predict front-to-front circles, if one allows that the multiply connected space has elliptic fixed-points. As another example, see the hyperbolic tetrahedral space investigated by Aurich (1999); Aurich & Steiner (2001).

Exploring all front-to-front circles with a HEALPIX resolution of  $N_{\text{side}} = 512$  we have not found any matched circle pair that can be significantly distinguished from false positive matches. The naive conclusion would be to announce that there are no matched front-to-front circles on the CMB sky. Maybe this conclusion is true, but care has to be taken since this conclusion has only little significance. The reason for the low significance is that the width of the  $D$ -value distribution, cf. Eq. (4), reaches the height of the  $D$ -values that are expected for matched circles, Eq. (3).

In order to be more specific, we make quantitative estimates for the width of the  $D$ -value distribution and for the height of the expected  $D$ -values in case of matched circle pairs. The height of the expected  $D$ -values for matched circles depends sensitively on the correlation ratio  $\chi$  of Eq. (5). The correlated signal in the CMB due to topology comes from the naive Sachs–Wolfe effect, only. Any other physical effects, e.g., the late integrated Sachs–Wolfe, the Doppler, and the Sunyaev–Zeldovich effect, contribute to the uncorrelated part of the signal. In addition, there are residual foreground contamination and detector noise which are not correlated with respect to the universal covering of the quotient space. Modelling the universe shows that the contribution of the late integrated Sachs–Wolfe effect plus the contribution of the Doppler effect is of the same order as the contribution of the naive Sachs–Wolfe effect, see fig. 8 in Aurich, Lustig & Steiner (2005b). This results in  $A_{\text{uncorr}}^2 + A_{\text{noise}}^2 \gg A_{\text{corr}}^2$ . Consequently, the correlation ratio is  $\chi \ll 1$ . If there would be a matched pair of circles in the sky, we would get a  $D$ -value for this matched circle pair which is  $D_{\text{peak}} \ll 0.5$ , see Eq. (3). These single  $D$ -values, one for each matched circle pair, are embedded in a large number of  $D$ -values that are distributed around  $D_{\text{peak}} = 0$  with a standard deviation of  $\sigma \simeq \sqrt{1/N_0}$ , cf.

Eq. (4). The largest number of independent pixels that a circle can sample in the *WMAP* data is  $N_0 = 360^\circ/0.23^\circ = 1565$  yielding  $\sigma \gg 0.025$ . Due to the large number of  $5 \times 10^{12}$   $D$ -values, namely one for each circle centre times each radius times each relative phase, many of these  $D$ -values reach  $D_{\text{max}} \gg 5\sigma \simeq 0.13$ . Among these  $D$ -values,  $D_{\text{max}} \gg 0.13$ , it might be possible to find a matched circle that has  $D_{\text{peak}} \ll 0.5$ , but the risk that matched circles are overlooked among many false positive detections is high. In particular, taking the detection threshold  $D_{\text{trigger}} \geq 0.3$  of Cornish et al. (2004) results in a number of false positive detections, whereas there is also the risk that even true matched circles may be missed, cf. Aurich et al. (2005c). Hence, the result so far of not having found any matched circles is not conclusive. Lowering or raising the detection threshold would lead to trouble, because of too many false positive detections or a too high risk of overlooking matched circles, respectively.

It has to be emphasized that the above estimates are rather optimistic. There might be additional physical effects and systematic errors that have an impact on the observed CMB. A slightly more pessimistic estimate on the correlation ratio  $\chi$  can worsen the above estimates seriously and  $D_{\text{peak}}$  may even drop below  $D_{\text{max}}$  making any detection of matched circles impossible.

## 6 CONCLUSION

Analysing CMB maps with  $D$  statistics allowed us to specify whether the available maps are contaminated by residual foregrounds. At the same time,  $D$  statistics highlighted the spatial resolution of the different CMB maps.

We conclude that, at present, the foreground cleaned  $Q$ -,  $V$ -, and  $W$ -band maps of Bennett et al. (2003) are the best available CMB maps of the full sky. The foregrounds in these maps have been removed with high quality outside the Kp2 mask. Even inside the Kp2 mask, but outside the Kp4 mask, the foreground reduction is very good. We recommend to use these maps in any quantitative analysis that allows the Kp4 mask to be applied. If one is cautious, it is safe to use the Kp2 mask combined with the point source mask.

Almost as well is the TOH map of Tegmark et al. (2003). If for some reason a quantitative analysis needs the full sky CMB map without any mask, we recommend to use the TOH map, instead.

We have searched for matched front-to-front circles, but have not found any. Combined with the results of Cornish et al. (2004) who have not found any back-to-back or nearly back-to-back circles, one could conclude that the universe does not possess a non-trivial topology. On the other hand, there are possible hints reported by Roukema et al. (2004); Aurich et al. (2005c) and the surprising anomalies in the large scale temperature fluctuations pointing towards a universe with non-trivial topology (de Oliveira-Costa et al. 2004). The contradiction may be due to the fact that the matched circles have all been overlooked. In particular, the answer to the title of the paper is that the existing CMB maps are not yet sufficiently accurate for the matched circle test to be conclusive. The question of the topology is still open, but with future observations of the CMB sky, we have the great hope to obtain the answer within the next decade.

## ACKNOWLEDGMENTS

I thank Dr. R. Aurich, S. Lustig, and Prof. F. Steiner for discussions and helpful comments. The use of the Legacy Archive for

## 6 *H. Then*

Microwave Background Data Analysis<sup>1</sup> (LAMBDA) is acknowledged. Support for LAMBDA is provided by the NASA Office of Space Science. The results in this paper have been derived using the CFITSIO<sup>2</sup>, the HEALPIX<sup>3</sup> (Górski, Hivon & Wandelt 1999), and the FFTW<sup>4</sup> (Frigo & Johnson 2005) libraries, the `gcc` compiler and `gnuplot`.

## REFERENCES

- Aurich R., 1999, *ApJ*, 524, 497  
Aurich R., Steiner F., 2001, *MNRAS*, 323, 1016  
Aurich R., Steiner F., Then H., 2003, in Bolte J., Steiner F., eds, Proc. International School on Mathematical Aspects of Quantum Chaos II. To appear in Lecture Notes in Physics, Springer-Verlag, preprint (gr-qc/0404020)  
Aurich R., Lustig S., Steiner F., Then H., 2004, *Class. Quant. Grav.*, 21, 4901  
Aurich R., Lustig S., Steiner F., Then H., 2005a, *Phys. Rev. Lett.*, 94, 021301  
Aurich R., Lustig S., Steiner F., 2005b, *Class. Quant. Grav.*, 22, 2061  
Aurich R., Lustig S., Steiner F., 2005c, preprint (astro-ph/0510847)  
Bahcall N. A., Ostriker J. P., Perlmutter S., Steinhardt P. J., 1999, *Science*, 284, 1481  
Bennett C. L. et al., 2003, *ApJS*, 148, 97  
Cornish N. J., Spergel D. N., Starkman G. D., 1998, *Class. Quant. Grav.*, 15, 2657  
Cornish N. J., Spergel D. N., Starkman G. D., Komatsu E., 2004, *Phys. Rev. Lett.*, 92, 201302  
de Oliveira-Costa A., Tegmark M., Zaldarriaga M., Hamilton A., 2004, *Phys. Rev. D*, 69, 063516  
Eriksen H. K., Banday A. J., Górski K. M., Lilje P. B., 2004, *ApJ*, 612, 633  
Frigo M., Johnson S. G., 2005, Proc. IEEE 93, 216  
Górski K. M., Hivon E., Wandelt B. D., 1999, in Banday A. J., Sheth R. K., Da Costa L., eds, Proc. MPA/ESO Conf., Evolution of Large-Scale Structure. PrintPartners Ipskamp, NL, p. 37  
Roukema B. F., Lew B., Cechowska M., Marecki A., Bajtlik S., 2004, *A&A*, 423, 821  
Tegmark M., Efstathiou G., 1996, *MNRAS*, 281, 1297  
Tegmark M., de Oliveira-Costa A., Hamilton A. J. S., 2003, *Phys. Rev. D*, 68, 123523  
Then H., 2006, in Cartier P., Julia B., Moussa P., Vanhove P., eds, *Frontiers in Number Theory, Physics, and Geometry*. Springer-Verlag, Berlin, p. 183

This paper has been typeset from a  $\text{\TeX}$ /  $\text{\LaTeX}$  file prepared by the author.

<sup>1</sup> <http://lambda.gsfc.nasa.gov/>

<sup>2</sup> <http://heasarc.gsfc.nasa.gov/docs/software/fitsio/>

<sup>3</sup> <http://healpix.jpl.nasa.gov/>

<sup>4</sup> <http://www.fftw.org/>